

Neutron Reflectivity Study of Thin Films of Hydrogen-Bonded Polymer Blends: Influence of Annealing on Composition Profile

Lei Jong, Eli M. Pearce, and T. K. Kwei*

Polymer Research Institute, Polytechnic University, Brooklyn, New York 11201

W. A. Hamilton, G. S. Smith, and G. H. Kwei

Los Alamos National Laboratory, Los Alamos, New Mexico 87545

Received April 15, 1991; Revised Manuscript Received November 13, 1991

ABSTRACT: We have investigated the plane average composition profile of a hydrogen-bonded polymer blend consisting of poly(styrene-*co*-vinylphenol), MPS-5, and deuterated poly(methyl methacrylate), d-PMMA. The results indicate changes in the composition profile after the thin film has been annealed at 170 °C. After annealing for 3 h, the initially homogeneous blend undergoes phase separation into a layer containing 68% (by volume) MPS-5 near the polymer/substrate interface and a layer dominated by d-PMMA at the air/polymer interface, with a broad region of concentration change in between. With further annealing, the d-PMMA-rich layer becomes thicker at the expense of the MPS-5 layer. After annealing for a total of 19.5 h at 170 °C and 7 h at 185 °C, the interface of polymer/air has a composition of 64% d-PMMA by volume while the polymer/substrate interface contains 70% MPS-5. The remixing of separated phases was caused by the degradation of MPS-5 as indicated by the GPC results.

Introduction

Recently, neutron reflectivity has been shown to describe the interface profiles of polymer blends with precision higher than what other techniques have achieved.¹ This method has been used to study block copolymers of polystyrene and poly(methyl methacrylate),² isotopic blends of polystyrene,^{3,4} polymer bilayers of chlorinated polyethylene/poly(methyl methacrylate),⁵ polymer bilayers of polystyrene/polystyrene-*d*,⁶ and polymer trilayers.⁷ The theoretical calculation of reflectivity spectra can be achieved by using an assumed composition profile and a multilayer algorithm.^{2,8} For example, the interface composition profile of an annealed bilayer of poly(methyl methacrylate) and polystyrene has been shown to have a hyperbolic tangent function.² The information of the average interface composition revealed by this technique would certainly contribute to the understanding of its role in the surface properties of these polymer blends. In particular, such an understanding is useful in devising ways to improve the surface properties such as wetting, friction, and adhesion.

The miscible blend under current investigation is composed of modified polystyrene and deuterated poly(methyl methacrylate) (d-PMMA). Polystyrene is modified to include a certain percentage of the vinylphenol unit; miscibility between the two polymers is achieved by the formation of hydrogen bonds between the vinylphenol units of MPS-5 and the ester group of d-PMMA. For example, polystyrene is not miscible with poly(methyl methacrylate) but becomes miscible when it is modified to contain ~5% of copolymerized vinylphenol units. Although the 5% modified polystyrene forms a single-phase blend with PMMA at room temperature, thermally induced phase separation can be seen at elevated temperatures. The thermally induced phase separation, commonly known as the lower critical solution temperature phenomenon, is reversible in many miscible blends; that is, the heterogeneous structure reverts to a single phase upon cooling. However, in a blend of 5% modified polystyrene and PMMA, light scattering results indicated that reversion to single phase was very slow and was not observed even when a slow cooling rate of 0.1 °C/min was

used. Because of this characteristic, the interface profile can be frozen easily after phase separation. The interface structure of these phase-separated blends reveals information which is relevant to the understanding of the role of specific interaction between two different polymers. Information about interfaces also has important applications in areas such as adhesion, where the bond strength depends, among other factors, on the penetration depth of adhesive molecules into the substrate.^{9,10}

It may be mentioned in passing that the thermally induced phase separation is completely inhibited below 200 °C and the significant change of the composition profile is not observed when the vinylphenol content in the copolymer exceeds about 10%. Neutron reflectivity studies of the latter blends will be described in a separate paper.

Experimental Section

The miscible blend consists of an equal weight of deuterated PMMA and poly(styrene-*co*-vinylphenyl) containing 5 mol % vinylphenol, designated in the text as MPS-5. Deuterated PMMA was purchased from Polymer Laboratory, Inc., and used as received. MPS-5 was prepared by the free-radical copolymerization of styrene and *p*-acetoxystyrene in dioxane at 60 °C for 17 h. The resulting polymer was precipitated in methanol and subsequently hydrolyzed with hydrazine hydrate. After hydrolysis, the solution was neutralized and filtered, and the polymer was again precipitated in methanol. The molecular weight and polydispersity of this polymer was characterized by GPC, and the density was measured by a floating method. The characteristics of MPS-5 and d-PMMA are summarized in Table I.

Thin films for neutron reflectivity studies were prepared by spin-coating a 3% toluene solution of the polymer blend onto a polished silicon disk (50-mm diameter, 7.5 mm thick) purchased from Semiconductor, Inc., Boston, MA. The film thickness was controlled by the spinning speed, ~2000 rpm in this case, and the viscosity of the solution. Because the exact thickness is not critical in this experiment, a rough estimate of the thickness was obtained from the known weight, density, and area of the film. The actual thicknesses, in the range 1200–1800 Å as determined later by neutron reflectivity, can be controlled by this simple method. The specimen was then placed in a vacuum oven at 100 °C for 3 days to remove the solvent. Neutron reflectivity spectra were measured on the same specimen before and after different stages of annealing.

Table I
Characteristics of MPS-5 and d-PMMA

polymer	M_n	M_w/M_n	density, g/cm ³	$b/V, \times 10^6 \text{ \AA}^{-2}$
MPS-5	84 900	1.70	1.0513	1.42
d-PMMA	87 500	1.03	1.2830 ^a	7.02

^a This value is obtained by using the density of h-PMMA (1.188 g/cm³) from Polymer Handbook and corrected for the 8% increase in the monomer mass.

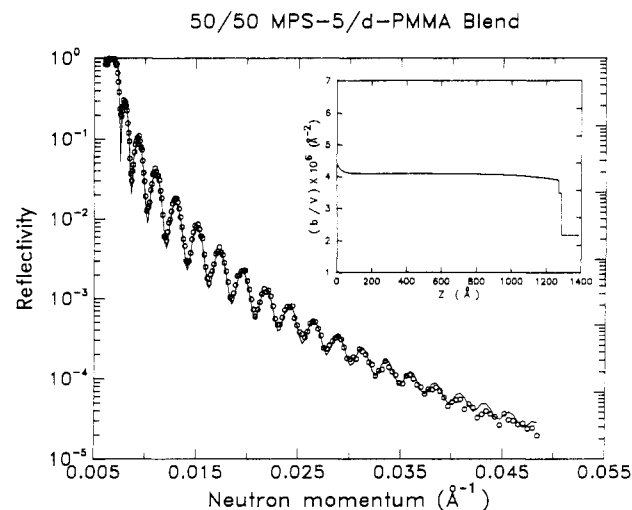


Figure 1. Experimental and calculated reflectivities for the sample before annealing. The circles are the measured data, whereas the solid line represents the calculated reflectivity using the scattering length density profile shown in the inset. The origin of the abscissa in the scattering length density profile is the air/polymer interface, with the substrate located at 1270 Å.

The neutron reflectivity experiments were performed on the reflectometer SPEAR at the Manuel Lujan, Jr., Neutron Scattering Center (LANSCE) at the Los Alamos National Laboratory. The nominal angle of incidence for these experiments was $\approx 1.0^\circ$, subject to the placement of sample. The incident and reflected beams define a vertical scattering plane. Using a temporary water moderator, we used a wavelength frame of $1 \text{ \AA} < \lambda < 16 \text{ \AA}$, which yields an accessible range of incident perpendicular wavevectors (at an incident angle of 1.0°) $0.007 \text{ \AA}^{-1} < k < 0.11 \text{ \AA}^{-1}$ where $k = 2\pi \sin(\theta/\lambda)$. Since the neutrons are generated by spallation, the neutron wavelengths were resolved using standard time-of-flight techniques. As defined by the detector resolution, the electronic timing resolution, and neutron pulse width, the resolution for these experiments was in the range $3\% < \delta k/k < 5\%$ for wavevectors ranging from 0.007 to 0.11 \AA^{-1} , respectively. With SPEAR in this configuration, the minimum measurable reflectivity is $R \approx 10^{-6}$. Typical counting times for these samples were approximately 3 h to obtain the statistics shown in Figures 1–4.

Results and Discussion

For an assumed composition profile, which is composed of $n + 1$ layers, including the substrate as the $(n + 1)$ th layer, the reflectance at the interface of the n th and $(n + 1)$ th layers is

$$R_{n,n+1} = \frac{k_n - k_{n+1}}{k_n + k_{n+1}} \quad (1)$$

where k_n is the neutron momentum in the medium n and is given by

$$k_n = [k_0^2 - 4\pi(b/v)_n]^{1/2} \quad (2)$$

and $(b/v)_n$ is the scattering length in the n th layer and k_0 the scattering vector perpendicular to the surface in vacuum (equal to $2\pi \sin(\theta/\lambda)$). After the calculation of reflectance $R_{n,n+1}$ for $n + 1$ layers, the reflectivity can be

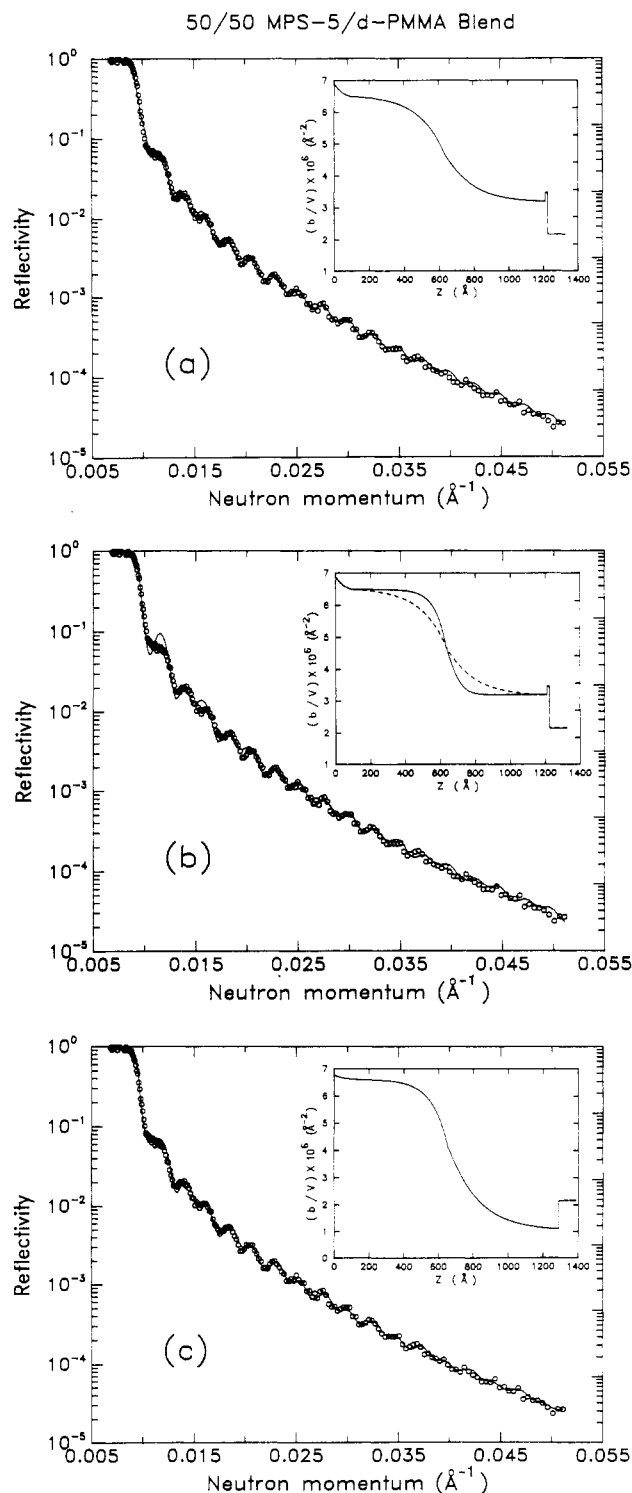


Figure 2. (a) Experimental and calculated reflectivities for the sample after annealing at 170°C for 3 h. The larger volume-averaged scattering length for the d-PMMA/MPS-5 blend near the air/polymer interface is readily evident. (b) This figure shows the change in the quality of fit due to the change in the composition profile. The dashed line is the profile used in a, and the solid line is the profile used in the calculation of the reflectivity shown in this figure. (c) This figure shows the assumed composition profile without a layer of silicon oxide.

obtained by the recursion formula^{2,8}

$$r_{n-2,n-1} = \frac{R_{n-2,n-1} + r_{n-1,n} \exp(2id_{n-1}k_{n-1})}{1 + R_{n-2,n-1}r_{n-1,n} \exp(2id_{n-1}k_{n-1})} \quad (3)$$

In this equation, d_{n-1} is the thickness of the $(n - 1)$ th layer

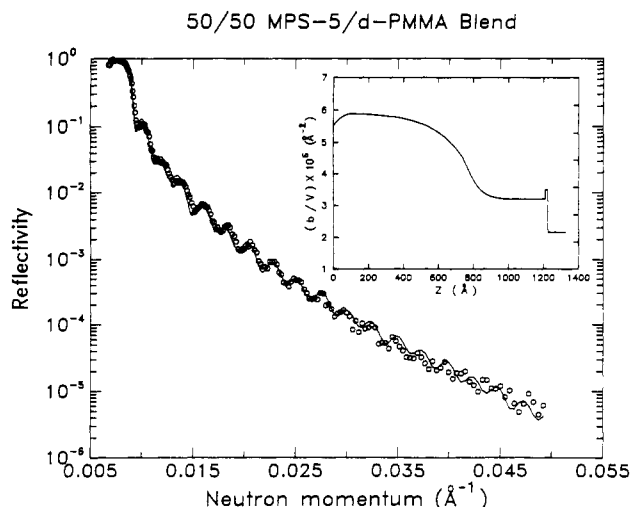


Figure 3. Experimental and calculated reflectivities for the sample after annealing at 170 °C for a total of 9 h. The solid line is the calculated reflectivity curve using the scattering length density profile shown in the inset.

and the reflectivity coefficient $r_{n-1,n}$ is given as^{2,8}

$$r_{n-1,n} = \frac{R_{n-1,n} + R_{n,n+1} \exp(2id_n k_n)}{1 + R_{n-1,n} R_{n,n+1} \exp(2id_n k_n)} \quad (4)$$

The recursion is continued until $r_{0,1}$ is obtained. Once $r_{0,1}$ is obtained, the reflectivity $R(k_0)$ is the complex product of $r_{0,1}$ and $r_{0,1}^*$. The roughness at the air/polymer and polymer/silicon interfaces can also be included in the recursion formulation. The plane average profile of roughness at interfaces is assumed to be a hyperbolic tangent;¹¹ the value of the roughness parameter presented in this paper is a parameter which characterizes, but is not equal to, the width of the hyperbolic tangent profile. Since we did not find a single mathematical function which can be used to describe the composition profile for these annealed blends, the combination of the exponential function and the modified hyperbolic tangent of the following forms is used. The choice of these functions is empirical and is not necessarily the only way to describe these profiles.

$$E(x) = \exp(-ax) \quad (5)$$

$$E(x) = E_0 + (H - E_0) (ae^{bx} - 1)/(ae^{bx} + 1) \quad (6)$$

In the above equations, a and b are adjustable parameters, E_0 is the average scattering length in the profile, H is the high limit of the scattering length in the profile, and

$$m = (x - n/2)d/D \quad (7)$$

where n is the number of layers, d the thickness of a single layer, and D the total thickness of the profile.

Usually, a thin film is first divided into two or three layers, and each layer is assigned a profile shown in eq 5 or 6. After that, each layer is again divided into a certain number of layers with 10–15 Å for each layer. With this approach, the fitting of reflectivity spectra is shown in Figures 1–4. Figure 1 shows the reflectivity of the sample before annealing, Figures 2 and 3 show the reflectivities after vacuum annealing at 170 °C for 3 and 9 h, respectively, and Figure 4 shows the reflectivity after annealing in vacuum for a total of 19.5 h at 170 °C and 7 h at 185 °C. The manipulation of the composition profiles near the air/polymer interface was done for a better fitting of intensity, especially at $k > 0.025 \text{ Å}^{-1}$. The fitting of the

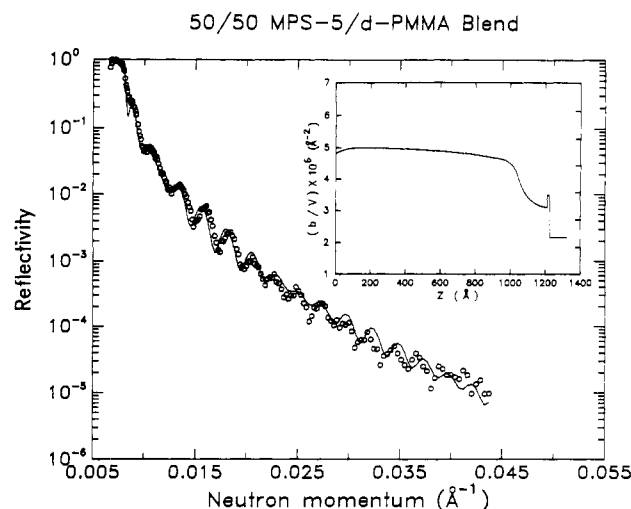


Figure 4. Experimental and calculated reflectivities for the sample after annealing at 170 °C for 19.5 h and at 185 °C for an additional 7 h. The growth of the width of the mixed polymer layer in the scattering length density profile from that shown in the inset of Figure 3 is readily evident.

Table II
Sample Thickness and Roughness Parameters at Different Stages of Vacuum Annealing

annealing condition polymer/substrate	film thickness, Å	roughness, Å	
		air/polymer	polymer/substrate
as-prepared	1270	4	13
3 h/170 °C	1230	6	13
9 h/170 °C	1230	10	13
19.5 h/170 °C and 7 h/185 °C	1240	10	13

intensity decay at this region is controlled by the parameter of the surface roughness and the profile near the air/polymer interface. However, the variation of the profile near the air/polymer interface in this case is small compared with that of the concentration gradient. Consequently, its contribution to the reflectivity is small. The film thickness and the roughness parameter at the interfaces for this specimen at different stages of annealing are summarized in Table II. It is seen that the surface becomes rough as the annealing time increases and the thickness of the film decreases by about 2.4% after the third and final annealing. The thickness of the film was determined by fitting the position of reflection maxima and minima. The calculated reflectivity profiles represent the best fit that we have attained through trial and error.

The as-prepared film has an almost uniform concentration profile throughout the thickness of the film as shown in the inset of Figure 1. Although d-PMMA and MPS-5 are expected to have different surface free energies, hydrogen bonding between the two polymers apparently is the dominant factor to result in an almost uniform concentration, except some slight excesses of d-PMMA and MPS-5 in the air/polymer and polymer/substrate interfaces, respectively. A 15-Å layer of silicon oxide is assumed to exist on the surface of the silicon substrate, but this assumption does not affect the fitting significantly. It is also noted that the average scattering length of this film is $4.1 \times 10^{-6} \text{ Å}^{-2}$, which is greater than $3.94 \times 10^{-6} \text{ Å}^{-2}$ calculated from the volume average of the individual components. This indicates the volume of the blend film is about 4% smaller than the sum of the volume of the individual components. A negative excess volume of mixing was also found from other hydrogen-bonded blends.¹²

After annealing in vacuum for 3 h at 170 °C, however, the film separates into a two-layer structure with a large concentration gradient of approximately 600 Å in width, as shown in the inset of Figure 2a, with the MPS-5-rich layer residing preferentially at the substrate and the d-PMMA-rich layer residing near the air interface. The cloud point of this particular blend is at about 130 °C, which is obtained from long time annealing (3 h at each temperature) in a vacuum oven. Because of the slow phase transition in this blend, the temperature scanning light scattering with a heating rate of 0.1 °C/min gives the cloud point which is 40 °C higher than that observed by long time annealing in the vacuum oven. From the cloud point we know that the annealing temperature, 170 °C, is well above the LCST and well within the two-phase region. At 170 °C the bulk sample was observed to become cloudy within 1 min. Therefore, the initial annealing for 3 h should have avoided the early stage of phase separation and have a minimum contribution from the off-specular reflection arising from the inhomogeneity in the lateral direction. Such inhomogeneity should diminish as the annealing time increases. The off-specular reflection is more significant at a high- q region, but we have chosen the q range such that the off-specular reflection is less than 6%, which is within the experimental error of the reflectivity. Other than that, they were subtracted together with the background in the raw data processing. At a smaller q region, $q < 0.035 \text{ Å}^{-1}$, the off-specular reflection was not observed from the two-dimensional reflectivity pattern. The inhomogeneity along the lateral direction, if there is any, cannot be obtained from the current analysis, as the composition profile is the result of a plane average profile.

Figure 2b shows the change of fitting due to the change in the assumed composition profile; this is to demonstrate how the change in the quality of the fit is affected by the change in the composition profile. Figure 2c shows an alternate fit without the assumption of a silicon oxide layer. The good fit from this profile indicates that more than one composition profile can be used to fit a set of reflectivity data. As a result, the choice of a suitable composition profile rests on the soundness of the assumptions used in the fitting. From the known knowledge that fresh-cut silicon is easily oxidized in air, it is logical to choose the composition profile which includes a layer of silicon oxide. In addition to this, the alternate profile without a silicon oxide layer results in the density of MPS-5 at the surface being 23% less than its bulk value, which is unreasonable. Therefore, the composition profile without a silicon oxide layer is ruled out.

Previously, Anastasiadis et al.² had found that in a phase-segregated diblock copolymer of deuterated styrene and methyl methacrylate, the deuterated polystyrene block preferentially stayed near the air/polymer interface; in a block copolymer of styrene and deuterated methyl methacrylate, the styrene block also preferentially stayed at the air/polymer surface. The contrasting behavior of MPS-5 is probably due to the interaction of MPS-5 with a silicon oxide layer through the hydrogen bond. A similar observation of the adsorption of alcohols onto the surface of silica was previously reported.¹³ The enrichment of d-PMMA on the air/polymer interface of this blend and the blends prepared from MPS containing 10% and 15%¹⁴ indicates the surface tension of the poly(styrene-co-vinylphenol) is greater than that of d-PMMA at 170 °C in vacuum. Considering the existence of a substantial contribution of the surface free energy at the air/polymer interface and the interaction free energy at the polymer/substrate interface to the total free energy of the thin film, the phase-separation process above the LCST is

Table III
Interface Compositions at Different Stages of Vacuum Annealing

annealing condition	interface composition ^a	
	air/polymer	polymer/substrate
before annealing	49/51	56/44
3 h/170 °C	2/98	68/32
9 h/170 °C	20/80	68/32
19.5 h/170 °C and 7 h/185 °C	36/64	70/30

^a This is the volume ratio right at the interfaces.

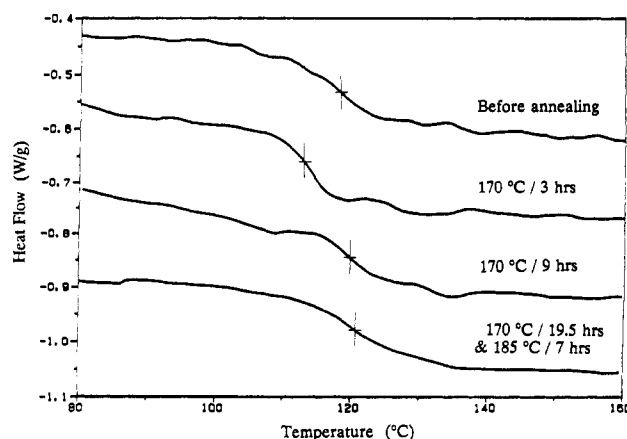


Figure 5. Glass transition temperatures of the blend annealed under various conditions. The shifting of T_g of a major phase in the blend can be seen clearly.

expected to be different from that in the bulk. As a consequence, the interface composition in the thin film cannot be identified as the composition of separated phases in the bulk sample. Also, due to these additional forces in the system, segregation should occur preferentially in the direction perpendicular to the substrate.

As the annealing time is increased to 9 h, the thickness of the MPS-5 layer decreases and that of the upper layer increases (Figure 3). After the final annealing at 185 °C for 7 h, the composition of the polymer/air interface changes to contain about 64% d-PMMA and the thickness of the top layer increases to about 900 Å (Figure 4). It appears that interdiffusion of the two layers has now enlarged the upper layer. The changes in the interface composition with respect to the annealing conditions are summarized in Table III. Interface compositions in terms of the volume ratio were estimated by assuming that the density of each component in the layer is the same as that of the pure component. The possibility that the remixing of separated phases is caused by the averaging process in the lateral direction is unlikely because the off-specular reflection arising from the inhomogeneity along the lateral direction cannot change the spacing between two adjacent reflection maxima significantly, while we observed such significant changes caused by the change in the thickness of top and bottom layers. The increasing thickness of the top layer is consistent with the lowering of its scattering length; therefore, the decrease of the reflectivity at the second and third annealing is not due to the off-specular reflection. In addition, by this time the inhomogeneity which causes the off-specular reflection must have become insignificant.

The study of the phase-separation process in the bulk was carried out with differential scanning calorimetry; the results are shown in Figure 5 and Table IV. We observed the shifting of T_g of a major phase in the blend. The trend is consistent with the observation from a thin film, but the phase compositions are different from that of a thin film.

Table IV
Glass Transition Temperature and Composition of a Major Segregated Phase in the Blend

annealing condition	T_g^a	composition
before annealing	115	50/50
3 h/170 °C	109	74/26
9 h/170 °C	117	44/56
19.5 h/170 °C and 7 h/185 °C	118	41/59

^a The T_g values have been corrected with the melting point of indium. The values listed here are about 3 °C lower than the transitions shown in Figure 5. The glass transition temperatures of MPS-5 and PMMA are 101 and 130 °C, respectively; all measurements are carried out with a heating rate of 20 °C/min.

Table V
Influence of Vacuum Annealing on the Molecular Weight and Polydispersity of PMMA and MPS-5

annealing condition	M_n	M_w/M_n
Poly(methyl methacrylate)		
before annealing	67 200	1.11
3 h/170 °C	54 700	1.12
9 h/170 °C	73 100	1.13
19.5 h/170 °C and 7 h/185 °C	76 400	1.20
Poly(styrene-co-vinylphenol)		
before annealing	57 400	2.04
3 h/170 °C	48 100	1.90
9 h/170 °C	36 500	2.36
19.5 h/170 °C and 7 h/185 °C	24 000	2.81

^a These are obtained from GPC measurements.

The phase compositions listed in Table V were estimated from an experimental curve of T_g versus compositions. In order to understand the annealing behaviors, we have investigated the possibility that degradation of PMMA and/or MPS-5 has occurred after annealing. The result of molecular weight and polydispersity of PMMA and MPS-5, after vacuum annealing, is listed in Table V. The molecular weight of MPS-5 before annealing in this table is smaller than that listed in Table I because of the reduction in the hydrodynamic volume of the chain caused by intrapolymer hydrogen bonds, while the molecular weight of MPS-5 in Table I is that of the precursor polymer. From this table, it is apparent that the molecular weight of PMMA is not decreased by the annealing, but a significant decrease of molecular weight and an increase of polydispersity is found in MPS-5. The decrease of the molecular weight of MPS-5 can certainly shift the LCST upward and lead to the remixing of separated phases. Apparently, this is mainly due to the small increase in the combinatorial entropy of mixing.

Although a number of theoretical predictions are available, both for the shape of a demixing interface and for its development with time, they are based on the Flory-Huggins type mean-field theory. The free energy of the hydrogen-bonded blend cannot be described by this theory.

However, the current analysis gives us a qualitative understanding of the change and the distribution of composition in a thin film of a hydrogen-bonded polymer blend under the effect of annealing. After the first annealing of 3 h at 170 °C, the inhomogeneity along the lateral direction would have become insignificant and the concentration gradient between the top and bottom layer would have approached or closely resemble the phase boundary in the thin film. This gives us a glimpse of the nature of the phase boundary in this blend.

In summary, the annealed thin film of a hydrogen-bonded polymer blend gives different compositions at its air/polymer and polymer/substrate interfaces. The surface composition and the surface properties of this blend change with the annealing condition due to the degradation of MPS-5. The phase boundary between two separated phases is generally broad and is on the order of several hundred angstroms (Figure 2a); the phase composition in the thin film is different from that in the bulk.

Acknowledgment. We acknowledge support from the National Science Foundation under Grant DMR 8820046. The neutron reflectivity experiments were carried out at the Manuel Lujan, Jr., Neutron Scattering Center at the Los Alamos National Laboratory, which is supported by the Department of Energy, Office of Basic Energy Sciences.

References and Notes

- (1) Russell, T. P. *Mater. Sci. Rep.* **1990**, *5*, 171.
- (2) Anastasiadis, S. H.; Russell, T. P. *J. Chem. Phys.* **1990**, *92* (9), 5677.
- (3) Composto, R. J.; Stein, R. S.; Jones, R. A. L.; Kramer, E. J.; Felcher, G. P.; Karium, A.; Mansom, A. *Physica B* **1989**, *156* and *157*, 434.
- (4) Jones, R. A.; Norton, L. J.; Kramer, E. J.; Composto, R. J.; Stein, R. S.; Russell, T. P.; Mansom, A.; Karium, A.; Felcher, G. P.; Rafailovich, M. H.; Sokolov, J.; Zhao, X.; Achwarz, S. A. *Europhys. Lett.*, in press.
- (5) Fernandez, M. L.; Higgins, J. S.; Penfold, J.; Shackleton, C. *Polym. Prepr. (Am. Chem. Soc., Div. Polym. Chem.)* **1990**, *31* (2), 71.
- (6) Stamm, M.; Reiter, G.; Huttenback, S.; Foster, M. *Polymer Prepr. (Am. Chem. Soc., Div. Polym. Chem.)* **1990**, *31* (2), 73.
- (7) Anastasiadis, S. H.; Menelle, A.; Russell, T. P.; Satija, S. K.; Felcher, G. P. *Polym. Prepr. (Am. Chem. Soc., Div. Polym. Chem.)* **1990**, *31* (2), 77.
- (8) Paratt, L. G. *Phys. Rev.* **1954**, *54*, 359.
- (9) Voyutskii, S. S. *Autohesion and Adhesion of High Polymers*; Kaganoff, S., Translator; Wiley-Interscience: New York, 1963.
- (10) Voyutskii, S. S.; Vakula, V. L. *J. Appl. Polym. Sci.* **1963**, *7*, 475.
- (11) Lekner, J. *Theory of Reflection*; Martinus Nijhoff Publishers: Dordrecht, The Netherlands, 1963.
- (12) Gsell, T. G.; Pearce, E. M.; Kwei, T. K. *Polymer*, to be published.
- (13) Hare, E. F.; Zisman, W. A. *J. Am. Chem. Soc.* **1955**, *59*, 335.
- (14) Jong, L.; Pearce, E. M.; Kwei, T. K.; Hamilton, W. A.; Smith, G. S.; Kwei, G. H., to be published.

Registry No. d-PMMA, 9011-14-7; (PS)(vinylphenol) (co-polymer), 72317-19-2.